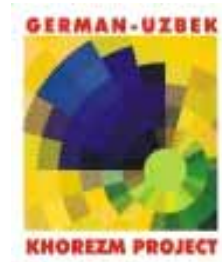




Zentrum für Entwicklungsforschung
Center for Development Research
ZEF Bonn

Economic and Ecological Restructuring of Land and
Water Use in Uzbekistan/Khorezm:
A Pilot Program in Development Research



ZEF Work Papers for Sustainable Development in Central Asia

No. 5

Exploring Leaf Area Index Development and Land Cover Classification in the Lower Amu-Darya Basin in Uzbekistan Based on Multi-Temporal and Multi-Spatial Remote Sensing Data

by

Gerd Ruecker¹ and
Christopher Conrad¹

¹German Remote Sensing Data Center (DFD) of the
German Aerospace Center (DLR), Oberpfaffenhofen,
82234 Wessling, Germany

Bonn, September 2003

ZEF-Uzbekistan working papers contain preliminary material and research results from **the ZEF/BMBF/UNESCO-Project on Economic and Ecological Restructuring of Land- and Water Use in the Region Khorezm (Uzbekistan)**. They are circulated prior to a peer review process to stimulate debate and to disseminate information as quickly as possible. Some of the papers in this series will be reviews and eventually be published in some other form, and their content may also be revised. The sole responsibility for the contents rests with the authors.

Project internet site: <http://www.khorezm.uni-bonn.de/>

**Исследование Развития Индекса Листовой Поверхности и
Классификация Землепользования в бассейне низовья Аму-Дарьи в Узбекистане на
основе Многовременного и Мультипространственного Дистанционного сбора данных**

**Герд Рюкер¹
и
Кристофер Конрад¹**

РЕЗЮМЕ

Неоднородное распределение воды в пространстве и во времени принято считать одной из главных причин серьезных проблем сельскохозяйственного производства на орошаемых территориях низовья реки Аму-Дарьи в Узбекистане. Для оценки воздействия неравномерного распределения воды на развитие растительности в течение 2002 года проводилось исследование по изучению фенологического развития при различных типах землепользования в этом регионе, с использованием временных рядов Индекса Листовой Поверхности (ИЛП) со спутникового датчика среднего разрешения Spectroradiometer (MODIS).

Различные пространственные модели максимальных, минимальных и других параметров развития ИЛП, а также девяти временных классов ИЛП были выделены и закартированы. Пространственные зависимости этих моделей ИЛП были найдены относительно их расположения вверх по течению или вниз по течению, а также расстояния от главных оросительных каналов. Ежегодная динамика ИЛП была охарактеризована более детально в пределах экологических единиц, которые представляют области с изменяющимся расстоянием до реки и оросительных каналов. Типичное развитие ИЛП, отражающее пространственное влияние этих водных источников, было идентифицировано для некоторых местоположений в этих единицах.

В дополнение к этим крупномасштабным исследованиям, было использовано много-спектральное спутниковое изображение Хорезмской области с высоким разрешением Landsat 7 ETM+, для установки связи ИЛП с определенными типами землепользования. Метод «отработанной» классификации выявило 13 классов использования земли, основанных на иерархической схеме классификации. Динамика ИЛП посевов риса и лесонасаждений была определена пространственными отношениями расстояния до реки и оросительных каналов, а также сгруппированными или рассеянными пространственными скоплениями такого вида землепользования. В отличие от этого, хлопковые и пшеничные поля, которые были широко рассеяны по области изучения, имели относительно однородную динамику ИЛП. На основе анализов исследования в региональном масштабе были выдвинуты гипотезы относительно специфичных для региона факторов, которые, возможно, определили эти различные пространственные и временные модели развития растительности, включая окружающую среду, управление и факторы инфраструктуры. Эти факторы могли бы быть более интенсивно исследованы, чтобы деятельно управлять и контролировать распределением ресурсов для оптимизированного производства культур в этой области.

TABLE OF CONTENTS

1	INTRODUCTION.....	1
2	METHODS.....	2
2.1	Conceptual Framework.....	2
2.2	Time-Series Analysis of MODIS Sensor Derived Leaf Area Index Products.....	3
2.2.1	MODIS Sensor Characteristics	3
2.2.2	Calculating Leaf Area Index Products from MODIS Sensor.....	3
2.2.3	Time-Series Analysis of Leaf Area Index.....	3
2.3	Supervised Land Cover Classification of Landsat-7 ETM+ Satellite Scene.....	4
2.3.1	Landsat-7 ETM+ Sensor Characteristics.....	4
2.3.2	Land Cover Ground Truthing.....	4
2.3.3	Supervised Land Cover Classification	5
2.4	Comparison of Leaf Area Index with Land Cover.....	5
3	RESULTS.....	6
3.1	Striking spatial patterns of leaf area index in the lower Amu Darya Basin in 2002.....	6
3.1.1	Absolute maximum leaf area index patterns	6
3.1.2	Absolute minimum leaf area index patterns.....	7
3.1.3	Leaf area dynamics patterns	7
3.1.4	Total annual leaf area turnover patterns	8
3.2	Temporal Patterns of Leaf-Area Index Time-Series.....	9
3.3	Spatial Patterns of Temporal Leaf-Area Index Time-Series.....	11
3.4	Example Spots for More Detailed Studies of LAI Patterns.....	12
3.5	Land Cover Classification.....	14
3.5.1	Level I - Land Cover Classification.....	14
3.5.2	Level II - Land Cover Classification.....	14
3.5.3	Level III - Land Cover Classification.....	16
3.5.4	Level IV - Land Cover Classification.....	17
3.6	Comparison of Land Cover Classes and LAI in Selected Spots.....	18
4	CONCLUSIONS AND OUTLOOK.....	19
	ACKNOWLEDGEMENTS.....	21
	REFERENCES.....	21

ABSTRACT

Spatially and temporally heterogeneous water distribution is assumed to be one of the major causes of the serious agricultural production problems in the irrigated areas of the lower Amu Darya River floodplains of Uzbekistan. In order to assess the impact of different water distributions on vegetation development this study investigated the phenological development of the different land covers in this region using Leaf Area Index (LAI) time-series data from the MODerate resolution Imaging Spectroradiometer (MODIS) satellite sensor for the year 2002.

Distinct spatial patterns of maximum, minimum and other LAI development parameters as well as nine temporal LAI classes could be separated and mapped within the floodplains. Spatial dependencies of these LAI patterns were found in relation to their upstream or downstream location, as well as in their distance from the main irrigation channels. Annual LAI dynamics were characterized in more detail within ecological units that represent areas with varying distance to the river and irrigation channels. Typical LAI developments, which mirrored the spatial influence of these water sources, were identified for certain locations in these units.

Complementary to these large-scale analyses, a high-resolution multi-spectral remote sensing Landsat 7 ETM+ satellite image of the Khorezm region was used to relate LAI to specific land cover types. The supervised classification revealed 13 land cover classes based on a hierarchical classification scheme. The LAI dynamics of rice and afforestations were determined by spatial distance relationships to river and irrigation channels as well as by clustered or dispersed spatial aggregation of these land uses. In contrast, cotton and wheat fields that were widely scattered over the study region had relatively homogenous LAI dynamics. Based on these regional scale explorative analyses, site-specific factors that may have determined these different spatial and temporal vegetation development patterns were hypothesized, including environmental, management and infrastructure factors. These factors could be more intensively investigated, in order to actively manage and control resource allocation for optimised crop production in this region.

1 INTRODUCTION

Embedded in the agro-ecosystems of the southern Aral Sea region and influenced by a strong continental climate, the water of the Amu Darya River is critical to life in the Khorezm and Karakalpakstan irrigation areas in Uzbekistan (UNESCO, 2000). The area of these irrigation systems has increased tremendously since the 1920s to support the demands for higher agricultural production of a constantly increasing population (Shirokova, 2000). Due to the relative upstream position of Khorezm this irrigation system has a comparative advantage in terms of water supply from the Amu Darya River compared to Karakalpakstan at a relative downstream position. Similar spatial dependence is likely to occur within each irrigation system between areas at the beginning and those at the end of the irrigation channels as well as between areas close to and more distant from the water supply.

One first approximation to explore water dependencies in these irrigation systems is to study how vegetation parameters change within systems in terms of spatial and temporal development patterns. The underlying assumption for this strategy of analysis is that water is a main factor in determining vegetation development patterns in irrigated systems. Vegetation parameters can be best studied for river basin agro-ecosystems using remote sensing techniques. The advantages of remote sensing techniques are that they offer large area observation with high frequency of image acquisition during vegetation cycles and publicly available vegetation parameter products. One frequently used vegetation parameter is leaf area index (LAI) that represents the plant canopy structure, which in turn can be understood as an indicator of varying water supply to vegetation (Myneni, 2002).

Modern remote sensing sensors like MODIS (Moderate Resolution Imaging Spectroradiometer) provide LAI products at high spatial coverage and high temporal resolution (Lotsch et al., 2001). Explorative trend analysis of a full year MODIS - LAI time series covering such a large agro-ecosystem is expected to produce a spatial and temporal perspective on the LAI development within that system. These first coarse-scale analyses may reveal major LAI patterns between upstream and downstream locations as well as within irrigation systems. These LAI patterns could then be further interpreted in terms of the specific land covers, which produced the respective LAI. The low spatial resolution of MODIS ground pixels can be compensated by integrated use of images from Landsat satellites, which have higher spatial resolution for usage in land cover studies. Those spatial and temporal pattern descriptions may lead to hypotheses about possible driving environmental (e.g. soil salinity), management (e.g. irrigation scheduling), or infrastructure (e.g. irrigation channel layout) factors determining vegetation and finally crop yield

development within the Amu Darya Basin. Hypotheses gathered during that explorative analysis might then be tested in subsequent research phases of the ZEF/UNESCO Khorezm project (Vlek et al., 2001).

The objectives of this study are 1) to explore and to describe the major spatial and temporal distribution of leaf area index (LAI) as one important ecological water related parameter in the lower Amu Darya Basin by using 2002 time-series satellite images; 2) to classify land cover by one Landsat-7 ETM+ satellite image covering most of the Khorezm region at a strategically selected acquisition date and to describe these land cover classes in term of their spatial pattern as well as spatial relationships to water bodies; 3) to compare LAI development patterns with the land cover classification pattern. Based on these steps, hypotheses will be formulated about possible driving factors of vegetation development within the Amu Darya Basin and to propose recommendations for water and land use management research in subsequent project phases.

2 METHODS

2.1 Conceptual Framework

The explorative analysis of leaf area index development and land cover classification was based on a conceptual framework. That framework combined remote sensing derived LAI and land cover information at multiple temporal and spatial scales.

High temporal scale LAI products with low spatial resolution were used to investigate LAI development for the lower Amu Darya Basin comprising both Khorezm and Karakalpakstan regions during the year 2002. This LAI development was analysed by descriptive statistics to identify major striking LAI patterns within the lower Amu Darya Basin. Based on the application of an unsupervised classification algorithm of LAI time-series, LAI classes with different LAI development cycles during 2002 could be distinguished. These LAI classes were mapped to demarcate respective spatial domains in the lower Amu Darya Basin.

More detailed analysis was performed in the Khorezm area. Example spots representing strong, moderate and weak annual LAI development were selected from the results of previous analysis and enlarged from those spatial domains of LAI classes that were within Khorezm. Information of LAI classes was related to descriptive LAI statistics in those spots. Image information from a different high spatial resolution satellite was used for supervised land cover classification according to a hierarchical classification. Land cover pattern was compared with LAI pattern in those spots to identify possible relationships. Secondary GIS data, such as hydrological network layout, were additionally used to interpret LAI patterns.

2.2 Time-Series Analysis of MODIS Sensor Derived Leaf Area Index Products

Leaf Area Index development was analysed using image products that were derived from the MODIS (*Moderate Resolution Imaging Spectroradiometer*) sensor onboard Terra satellite. The specific characteristics of the MODIS sensor, the leaf area index product and the time series analysis are described in the following.

2.2.1 MODIS Sensor Characteristics

MODIS images the earth with a swath width of 2,330 km. For the purpose of this study a spatial subset was clipped out with the dimensions ULX=11085900, ULY=4922740, LRX=11462900, LRY=4480740. MODIS acquires images every eight days. Three scenes of the annual acquisition series were not recorded for that subset during 2002 due to satellite problems. These scenes covered the dates 21.03.02, 26.06.02 and 27.12.02. The actual time series available consisted of 43 scenes. The spectral resolution of MODIS captures 36 spectral bands ranging from 0.405 to 14.385 μm in wavelength. Leaf area index is a product that is calculated from MODIS spectral bands and validated by ground truthed test sites on an operational basis.

2.2.2 Calculating Leaf Area Index Products from MODIS Sensor

LAI is a standard product derived from MODIS spectral bands at a spatial resolution of 1 km. LAI is defined as the one sided green leaf area per unit ground area in broad leaf canopies and as the projected needle leaf area in coniferous canopies. MODIS LAI products are modelled in a synergistic algorithm, which incorporates surface reflectance, land cover and cloud state image data (Knyazikhin, et al., 1998). The LAI outputs are validated based on global biomes (Lotsch et al., 2001).

2.2.3 Time-Series Analysis of Leaf Area Index

All 43 LAI products were imported into Erdas Image analysis software and processed to a composite LAI image layer stack. This composite image was georeferenced to Transversal Mercator projection, Krasovsky Spheroid and Pulkovo 1942 Datum. The analysis of LAI comprised two main steps:

- 1) Different descriptive statistics were performed on this time series. Statistics comprised calculation of maximum, minimum, summation and dynamics (count of LAI value changes at each pixel over time) of LAI values. The spatial representation of results from these statistics was mapped.

- 2) Unsupervised classification was performed on the LAI time-series data to distinguish LAI classes with different LAI development cycles during 2002. Mean and standard deviation of resulting LAI classes were calculated for each image acquisition time step and graphically displayed. The flow of these class specific graphs was interpreted in terms of LAI temporal development over 2002. LAI classes were mapped to demarcate respective spatial domains.

More detailed analysis was performed in the area of Khorezm, where LAI patterns were related to land cover information.

2.3 Supervised Land Cover Classification of Landsat-7 ETM+ Satellite Scene

Supervised classification of land cover in Khorezm and part of surrounding area was performed using one image of Landsat-7 ETM+ sensor and intensive ground truthing information. The Landsat characteristics, ground truthing and classification strategy are documented in the following sections.

2.3.1 Landsat-7 ETM+ Sensor Characteristics

Landsat-7 ETM+ (*Land Satellite Enhanced Thematic Mapper Plus*) acquires images from the earth with a swath width of 185 km. Due to the path and row orientation of this satellite the Khorezm region cannot be captured by one scene, which cuts off parts of the upstream Pitnak District area. Landsat-7 ETM+ sensor scans every single point on earth every 16 days. However, the satellite operator determines the image acquisition rate according to priority setting of a long-term acquisition plan, which usually results in an acquisition time of a multiple of 16 days. The spectral resolution of Landsat-7 ETM+ consists of eight bands ranging from 0.45 – 12.5 μm wavelength. Land cover can be identified and classified from the spectral information of Landsat-7 ETM+ images by ground truthing land cover in training areas as simultaneously as possible with image acquisition.

2.3.2 Land Cover Ground Truthing

The time period for the fieldwork and the acquisition of the Landsat-7 ETM+ image in 2002 was chosen to coincide with the period before winter wheat would be harvested and after planted cotton and rice have emerged from the ground. Due to the long 2002 winter and persistent cold temperatures in the Khorezm region the target time period was reached by mid June. The field survey to ground truth different land cover (LC) types lasted from the 16th June 2002 until the 24th June 2002. The acquisition date for Landsat-7 ETM+ images that was temporally closest to this ground truthing time period was 12th July 2002.

A previous literature review on the different land cover types in the Khorezm region was used to develop a potential LC type classification system. This classification system was generated in hierarchical levels according to most recent internationally established classification standards (FAO, 1997; Jansen and Gregorio, 2002). Training areas, which identify representative LC sites according to this classification system were randomly selected right and left from roads traversing Khorezm region. A detailed questionnaire was established based on information gathered during two field pre-tests, from local expert consultants and a literature review. The questionnaire was elaborated to capture the characteristic ecological parameters of LC types. Besides the information describing LC the questionnaire contained fields for entering the geographic position of training sites. Geographic position was measured by handheld GPS. Three teams carried out the ground truthing simultaneously. By using this survey strategy temporal sampling bias could be avoided. Descriptive information about training sites in the questionnaire was entered into a MS Access database. Geographic information on the location of the training sites was downloaded from the GPS. Both descriptive and geographical information were imported into ArcView GIS 3.3 and combined in one GIS data set, which in turn was used in the supervised land cover classification.

2.3.3 Supervised Land Cover Classification

The Landsat-7 ETM+ image was imported into Erdas Imagine Image processing software and georeferenced using 48 ground control points, which were measured by handheld GPS in the middle location of street crossings of Khorezm region. The GIS LC training areas were overlaid on the Landsat-7 ETM+ image and used to demarcate spectrally homogenous training areas for each LC type on the satellite image. Spectral signatures of these homogenous training areas were then transferred to a spectral signature editor. Supervised classification was performed for the image by applying a maximum likelihood algorithm. This algorithm is based on the probability that a pixel belongs to a particular class. The basic equation assumes that these probabilities are equal for all classes, and that the input bands have normal distributions (Freund, 1992):

2.4 Comparison of Leaf Area Index with Land Cover

Land cover pattern was compared with LAI pattern in example spots to identify possible relationships. Secondary GIS data, such as hydrological network layout and groundwater salinity changes, were additionally used to interpret LAI patterns.

3 RESULTS

Spatial and temporal patterns of leaf area index covering the lower Amu Darya Basin will be presented in the following. Land cover classes of Khorezm will be explained and relationships between leaf area index and land cover classes will be drawn. These results will highlight possibilities of relating LAI and land cover information with other ground information such as the irrigation channel network. Finally it will be shown how time series analysis of LAI and land cover information can be used as a first step towards monitoring vegetation and water distribution.

3.1 Striking spatial patterns of leaf area index in the lower Amu Darya Basin in 2002

The explorative statistics of LAI time series and unsupervised classification revealed different spatial patterns that will be explained in the following.

3.1.1 Absolute maximum leaf area index patterns

The spatial patterns of absolute maximum LAI values during 2002 were striking in three locations of the lower Amu Darya Basin (Figure 1¹). These locations comprised:

- 1) the upstream area that is directly adjacent to the river and patterns that extended from the river
to the northwest into the irrigation zone (maximum LAI values ca. 6.0 – 7.0);
- 2) the midstream area, in which only few patches of high maximum LAI values (ca. 6.0) were surrounded by medium level LAI maximum (ca. 2.0 – 4.0);
- 3) the downstream area in Karakalpakstan, where the flow of the Amu Darya turns northward (ca. 6.0 – 7.0);

These maximum LAI values show the maximum photosynthetic activity in an area of 1 km² over the whole of 2002. The high LAI maxima in downstream and upstream areas can be interpreted to represent ecosystems with high photosynthetic activity during at least one time step over the year. Low maxima may demarcate areas with no or little green vegetation cover during the whole year.

¹ All figures are located in an additional PDF file available from www.khorezm.uni-bonn.de

3.1.2 Absolute minimum leaf area index patterns

The analysis of the absolute minimum LAI during 2002 revealed the following remarkable spatial patterns (Figure 2): These spatial patterns were found in:

- 1) the very upstream area and part of the midstream area with lowest LAI values (0.0) and some few patches of low LAI (ca. 0.1);
- 2) the northern part of the midstream area that is characterized by the highest minimum LAI values (ca. 0.2 - 0.3);
- 3) the lower downstream area adjacent to the Aral Sea with lowest LAI minimum values (0.0)

The spatial pattern of the minimum LAI corresponds to areas where photosynthetic activity is low during at least one time period of 8 days in the whole Amu Darya Basin. Although the legend in figure 2 indicates a certain range of LAI, values of LAI that are lower than 0.4 do not in fact consist of any green vegetation. Maximum and minimum LAI measures represent only the extreme LAI values during the year. The characteristic temporal development of vegetation during the year cannot be captured by these measures.

3.1.3 Leaf area dynamics patterns

One possible way to investigate LAI dynamics is to count how often the LAI value changes from one time-period to the next during a whole year. The major spatial pattern of LAI dynamics follows a similar pattern to that of the LAI maximum (Figure 3).

The highest LAI dynamics were observed in two areas:

- 1) the upstream area in central Khorezm, directly adjacent to the river and extending to the northwest (20-24 different LAI values);
- 2) the downstream area in Karakalpakstan directly adjacent to the river (25-29 different LAI values).

The lowest LAI dynamics are located in three areas:

- 1) the midstream area where Khorezm connects to Karakalpakstan (0-14 different LAI values);
- 2) the eastern part of the downstream area in Karakalpakstan (0-19 different LAI values);
- 3) the branch-like patterns that extend from the Karakum desert in a south-easterly direction into the irrigated areas of both Khorezm and Karakalpakstan (4-9 different LAI values).

In the irrigated zone of the lower Amu Darya Basin the LAI dynamic decreases from areas close to the river to areas that are located in more far distance. This phenomenon might be explained in that areas close to the river may experience higher water supply, and thus may have more accelerated leaf growth, which in turn increases LAI dynamics. On the other hand, increasing distance to the river might lead to reduced water availability for vegetation, which might force slow or stunted vegetation growth, thus resulting in lower LAI dynamics values. Although the dynamics of LAI values relates to the intensity of the vegetative growth process, this measure is limited to differentiating between areas of high LAI dynamics that accomplish their high value during the whole vegetation period or only during a shorter time period. Further exploratory statistics of LAI values that account for the total LAI amount during the whole year is expected to overcome this limitation.

3.1.4 Total annual leaf area turnover patterns

The summation of the LAI values during 2002 can be used as an indicator to compare the total LAI turnover during the cycle of a year. Within the irrigated zone of the Amu Darya Basin three major areas can be distinguished that are displayed in Figure 4.

The highest annual LAI turnover patterns are striking in two areas:

- 1) the upstream area where spatial patterns with maximum LAI summation values range from 41 to 80. These spatial patterns can be found adjacent to the river and along a northwest branch;
- 2) the downstream area which contains the largest patterns with highest LAI summation values ranging from 81 to 120. These patterns are located directly adjacent to the river and stretching towards the desert fringe. The northern part of this area shows northward-reaching branches with high LAI summation values and one patch representing very high LAI summation values in the northwest corner of the irrigated zone.

The medium annual LAI turnover patterns are indicated mainly in the midstream area (summation values of 21-40). The lowest LAI turnover patterns occur in branchlike patterns entering in that midstream area (summation values of 20 or below).

A final interpretation of the LAI summation shows LAI patterns that are richer in contrast, and thus sharpen the spatial demarcation of previous patterns gained from LAI maximum, minimum and LAI dynamics statistics.

There are different limitations for an accurate interpretation of these LAI values. If for example the 1 km² pixel resolution of MODIS sensor covers a ground area with heterogeneous vegetation types, the corresponding LAI value would reflect the average multi-spectral LAI value of all vegetation types in that ground area. In that case vegetation types that cover high LAI values in a small fraction of the total pixel area would be less represented in the resulting LAI value. Another limitation is that the descriptive statistics process the information from all time steps of the year 2002 together, but related time information is not captured; i.e. it is not clear when certain LAI maximum or dynamics occurred. Investigation of the temporal LAI pattern might overcome the time related limitations.

3.2 Temporal Patterns of Leaf-Area Index Time-Series

The analysis of temporal LAI development is expected to reveal important information about the cycle of vegetation during a year, which again may help to better characterize vegetation dynamics. Unsupervised classification of 43 LAI time series images resulted in nine distinct LAI classes (Figure 5). Mean and standard deviation LAI values of each class were investigated for each time period of the year 2002. The date ranges for specific temporal patterns such as striking peaks and slopes of each class are summarized in Table 3.1.

Table 3.1: Temporal patterns of LAI characteristics in different LAI classes

Class #	Time Step	Date Range	LAI Values	Development	Temporal LAI Pattern
				Tendency	
				0=stagnant	
				+ =increase	
				++=strong increase	
				- =decrease	
				--=strong decrease	
Class 1	1 – 43	Whole year 2002	ca. 0.2	0	Very low LAI , relative steady state
	1 – 20	01.01. – 10.06.	ca. 0.2	+	Very low LAI, soft increasing
Class 2	21 - 43	18.06. – 19.12.	ca. 0.4	0 / -	Very low LAI
	1 – 10	01.01. – 14.03.	ca. 0.2	0	Very low LAI
	11 - 25	22.03. – 28.07.	ca. 0.2 – 1.0	+	Very low LAI, steady increase to low LAI
Class 3	26 – 37	05.08. – 01.11.	ca. 1.0	0	Low LAI
	38 – 43	09.11. – 19.12.	< 1.0	-	Low to very low LAI
	1 – 10	01.01. – 14.03.	ca. 0.2	0	Very low LAI
	11 – 22	22.03. – 04.07.	ca. 0.2 – 1.2	+	Steady increasing to low LAI
Class 4	23 – 28	12.07. – 21.08.	ca. 1.2 – 3.0	++	Sharper increasing to a peak at medium LAI
	29 – 35	29.08. – 16.10.	ca. 3.0 – 1.0	--	Strong decreasing to low LAI
	36 – 43	24.10. – 19.12.	ca. 1.0 – 0.2	-	Soft decreasing to very low LAI
	1 – 10	01.01. – 14.03.	ca. 0.2	0	Very low LAI
	11 – 20	22.03. – 10.06.	ca. 0.2 – 1.0	+	Soft increasing to low LAI
Class 5	21 – 29	18.06. – 29.08.	ca. 1.0 – 4.6	++	Sharp increasing to high LAI
	29 – 35	06.09. – 16.10.	ca. 4.0 – 1.0	--	Strong decreasing to low LAI
	36 – 43	24.10. – 19.12.	ca. 1.0 – 0.4	-	Soft decreasing to very low LAI
	1 – 10	01.01. – 14.03.	ca. 0.2	0	Very low LAI
	11 – 20	22.03. – 10.06.	ca. 0.2 – 1.0	+	Soft increasing to low LAI
Class 6	21 – 29	18.06. – 29.08.	ca. 1.0 – 4.6	++	Sharp increasing to high LAI
	29 – 35	06.09. – 16.10.	ca. 4.0 – 1.0	--	Strong decreasing to low LAI
	36 – 43	24.10. – 19.12.	ca. 1.0 – 0.4	-	Soft decreasing to very low LAI
	1 – 10	01.01. – 14.03.	ca. 0.2	0	Very low LAI
	11 – 21	22.03. – 18.06.	ca. 0.2 – 1.1	+	Medium increasing to low LAI
	22 – 24	26.06. – 20.07.	ca. 1.0	-	Medium LAI
Class 7	25 – 34	28.07. – 16.10.	ca. 1.0 – 3.0	++ / --	Medium LAI with two maxima (ca. 3.0)
	35 – 41	24.10. – 03.12.	ca. 1.0	0	Lower LAI
	42 – 43	11.12. – 19.12.	ca. 1.0 – 4.0	++	Sharp increasing LAI
	1 – 30	01.01. – 06.09.	ca. 0.2 – 1.5	+	Steady increasing LAI
Class 8	31 – 36	15.09. – 24.10.	ca. 1.5 – 4.3	++	Sharp increasing with a break at medium LAI (ca. 2.5) at 30.09.
	37 – 40	01.11. – 25.11.	ca. 4.3 – 0.5	--	Sharp decreasing to very low LAI

	1 – 10	01.01. – 14.03.	ca. 0.2	0	Very low LAI
	11 – 21	22.03. – 18.06.	ca. 0.2 – 1.0	+	Steady increasing to low LAI
Class 9	22 – 40	26.06. – 25.11.	ca. 1.0	0	Low LAI
	41 – 43	03.12. – 19.12.	ca. 1.0 – 3.5	++	Strong increasing

Based on the analysis of temporal LAI patterns (Figure 5 and Table 3.1), LAI classes can be summarized in three distinct groups:

- 1) The first group comprises LAI classes with low LAI values that develop little and remain almost constantly low during the whole year. For further reference that group was named “*Whole year low LAI development*”. The LAI development of this group corresponds mainly to the classes 1, 2 and 3.
- 2) The second group is characterized by a sudden sharp increase of LAI values between the end of June and the beginning of July reaching highest LAI values at the end of August. That group was named “*Mid year peak LAI development*”. The temporal LAI pattern of this group matches best with the dynamics of LAI classes 4, 5 and 6.
- 3) The third group has high maxima similar to those of group two; however group three is distinguished from group two because high LAI values occur later during the year, between the middle of September and December. That third group was called “*End year peak LAI development*” and comprised the classes 7, 8 and 9.

3.3 Spatial Patterns of Temporal Leaf-Area Index Time-Series

The temporal LAI development can be demarcated by spatial LAI pattern (Figure 6):

- 1) Classes 1 to 3 comprise mainly desert areas, the midstream part that connects the irrigated areas of Khorezm and Karakalpakstan as well as the fringes of the higher LAI classes. More specifically class 1 occurs predominantly in the desert areas of Karakum and Kyzylkum. Class 2 can be mainly found in the desert fringe of the irrigated area and in the branches ranging from the desert into the irrigated area. Class 3, which shows pixels of similar LAI values in larger clusters, dominates the fringes where the irrigated area connects to the desert as well as the midstream area of the delta close to the river.
- 2) Classes 4 to 6 are mainly located close to the river or major irrigation channels, in much of Khorezm and Karakalpakstan’s irrigated areas. Class 4 and class 5 are located in the surroundings of the Amu Darya in the downstream and the upstream areas as well as

surrounding the main irrigation channels that branch off in North-West Direction from the Amu Darya. The spatial location of class 6 mainly demarcates areas that are directly adjacent to the river, predominantly in the downstream area of Karakalpakstan.

- 3) Classes 7 to 9 can only be found in the transition zone from irrigation area to natural land downstream of Amu Darya in Karakalpakstan. The last three classes are highly fragmented. They can mainly be found in the northern part of the downstream area (Amu Darya delta) towards the Aral Sea.

Although these LAI descriptions revealed the major spatial and temporal LAI class distribution within the lower Amu Darya Basin, small-scale LAI variations could not be captured. More intensive analysis such as in actively selected example spots might be promising to study especially the small-scale spatial relationship of certain LAI classes with neighbouring LAI classes and to explore possible spatial relationships with the Amu Darya River or the main irrigation channels.

3.4 Example Spots for More Detailed Studies of LAI Patterns

Based on the unsupervised classification, explorative statistics and time series analysis, eight example spots with strong, moderate and weak annual LAI development were actively selected for more in-depth analysis of LAI patterns. The boundaries of these spots are indicated in Figure 7. Spots 1-4 are located in the upstream area of the lower Amu Darya Basin traversing Khorezm region from the desert fringe (spot 1) over the central irrigation area (spot 2), over the area close to the Amu Darya river (spot 3) to the area that is directly adjacent to the river (spot 4). Spots 5 and 6 represent striking LAI development sites in the middle part and spots 7 and 8 sites in the lower part of the Amu Darya basin. The LAI spatial patterns from unsupervised LAI classification and LAI dynamics are enlarged and displayed in Figures 8-11. The most dominant LAI classes and LAI dynamics in these spots are presented in Table 3.2.

Table 3.2: LAI class distribution and LAI dynamics in example spots

Spot #	Spatial Location	LAI Class Distribution	LAI Dynamics
1	Upstream; fringe between desert and Khorezm irrigated zone	Transition zone (SE-NW direction) from class 1 to class 2; fragmented patterns of classes 2, 3 and 4	In SE-NW direction: Very little (0-3) to little (4-9) dynamics; some fragmented high (20-24) and high-to-moderate (15-19) patterns of LAI dynamics
2	Upstream; central area of Khorezm irrigated zone	Transition zone (SE-NW direction) including class 4-3-2-1-2-3-4; fragmented patterns of class 5	In SE-NW direction: High-to-moderate (19-15) to moderate (14-10) and little (9-10) LAI dynamics and vice versa
3	Upstream; surrounds the beginning of the main irrigation channel; close to river; within Khorezm irrigated zone	Approximately equal contribution of class 5 and 4; fragmented patterns of class 3	Approximately equal contribution of high (20-24) and high-to-moderate (19-15); some few fragmented patterns of moderate (10-14) LAI dynamics
4	Upstream; directly adjacent to river; within Khorezm irrigated zone	Predominantly class 5; fragmented patches of class 4 as well as of class 6	Approximately equal contribution of high (20-24) and high-to-moderate (19-15) patterns of LAI dynamics in clusters parallel to the river
5	Midstream; directly adjacent to river; adjacent to Khorezm irrigated zone	Dominance of class 3 followed by class 4 and class 5	Approximately equal contribution of high-to-moderate (19-15) and moderate (14-10) patterns of LAI dynamics; high (20-24) LAI development in patches;
6	Midstream; directly overlapping river within Karakalpakstan	Transition zone (SE-NW direction) from class 1 to class 3 pattern; fragmented patterns of class 2	In SE-NW direction: Little (4-9) to moderate (10-14) to moderate-to-high (15-19) transition of LAI dynamics
7	Downstream; at the Eastern fringe of the irrigated area; within Karakalpakstan	Fragmented patches of classes 4-9 surrounded by clusters of class 3	Fragmented patches of high (20-24) surrounded by moderate-to-high (15-19) and moderate (14-10) LAI dynamic patterns
8	Downstream; at the western fringe of irrigated area; within Karakalpakstan	Dominance of clustered class 8 with smaller class 6 cluster in the center, surrounded by fragmented patches of class 9, 2 and 5	High (20-24) and highest (25-29) LAI dynamics in the center, surrounded by moderate-to-high (15-19) and moderate (14-10) LAI dynamic patterns

These results show that certain LAI classes and LAI dynamics were typical for certain locations in a regional perspective, e.g. LAI classes 1 and 2 and mainly low LAI dynamics were typical for areas close to the desert (spot 1). In contrast, LAI classes 3 and 4 as well as high LAI dynamics were mainly located in areas close to the river and surrounding the main irrigation channels (spot 4). A mixture of LAI classes 1-4 and LAI dynamics ranging from low to high could be traced along a distinct SE-NW gradient direction in the centre of the irrigated area of Khorezm (spot 2).

For better interpretation of LAI patterns in terms of the specific vegetation types, which produce the LAI classes and dynamics, the respective land cover was classified.

3.5 Land Cover Classification

Land cover classes of the hierarchical land cover classification scheme (Figure 12) were compared with the results from the land cover classification (Figure 13). Congruences and dissimilarities of this comparison are discussed in the following:

3.5.1 Level I - Land Cover Classification

Land and water classes could clearly be distinguished on the satellite image at LC level I. Water (blue pixels in the overall classification map (Figure 13)) could be mainly found in the centre and south of the image, comprising Amu Darya River (Spot 4 in Figure 14, Spots 5 and 6 in Figure 15) and lakes (Spots 1 and 2 in Figure 14).

3.5.2 Level II - Land Cover Classification

Land class: At level II zones of this land class comprising the irrigation zone (brown, pink, red and orange signatures), the natural zone (yellow, greenish yellow and three green signatures) and the settlement and infrastructure zone (greyish LC class) could be significantly demarcated on the satellite image (Figure 13). The irrigated zone was adjacent to the river, while natural zones comprised the desert (Spot 1 in Figure 14) as well as some niche positions in the direct vicinity of the river (Spots 5 and 6 in Figure 15). The settlement and infrastructure class has been detected with great confidence as major town clusters within the irrigated zone (e.g. Spot 1 in Figure 14).

However, the same greyish signature as for settlements and infrastructure can be also found North of Amu Darya River in areas at the desert fringe, where no major town clusters are located (Spot 5 in Figure 15). The surface of this desert fringe might have consisted of a geological rock type similar to spectral signatures of settlement and infrastructure. The definite identification and discrimination of this area is not possible with the present data and information available, because the specific spectral signature of that desert fringe was not collected during the ground truthing campaign, which focused on the Khorezm region, south of the Amu Darya river.

Water bodies. The extraction of water classes at level II revealed clear results for river, lake and major drainage and irrigation objects, but not for wetlands. Detailed multi-spectral investigation of the river object indicated that this class did not show a homogenous multi-spectral signal, but significant differences of the river signature. Among the main spectral signature (dark blue colour) of the upstream Amu Darya area, some single small patches with brighter reflectance values than the surrounding, main spectral signature of the river could be detected (brighter blue colour) (Spot 4 in Figure 14 and Spot 5 in Figure 15). The spatial occurrence of these brighter reflectance values increased further towards mid-stream areas. Following the flow of the river further downstream, the

spectral composite of the river changed abruptly after the river passed the main irrigation zone of the Khorezm region (Spot 5 in Figure 15). In the following course of the river, the multi-spectral satellite signal of the river signature was continuously dominated by the bright reflectance values (Spot 6 in Figure 15).

These clear spatial occurrence and changes of dominance of the brighter reflectance values compared to those darker reflectance values may exhibit some significant inter-relationship to processes that were connected with these adjacent land areas, depending on whether these land areas were irrigated or non-irrigated. Differences in multi-spectral river reflectance values could have occurred due to siltation from agricultural fields into the river. Silt-enriched water might have produced stronger multi-spectral reflectance in river areas that were adjacent to the irrigation zones, while little or no siltation in the river along non-irrigated areas further downstream might have produced a brighter spectral signal. Another possible hypothesis for this phenomenon might be the influence of salt loaded water from agricultural fields that has been entered the river downstream from the irrigation zone. This salt-loaded water might serve as a tracer and produce a brighter multi-spectral river colour than the surrounding river water.

Possible strategies to test these hypotheses include for example the investigation of water samples that could be taken at different river positions or the tracing of the flow of salt-enriched drainage water from the fields through the drainage network. A third option might be to acquire satellite images that cover further upstream river areas with adjacent non-irrigated areas. In these upstream river areas it is expected that a similar spectral signature to those non-irrigated areas further downstream will be identified. Systematic ground data collection is therefore necessary to identifying the exact causes of that phenomenon and to validate satellite image classes.

Drainage and irrigation channels could be identified on the image and differentiated from other water classes as long as these channels had a certain minimum spatial dimension, e.g. linear structures crossing the desert in the south and linear features branching off the river Amu Darya (e.g. Spots 2, 3 and 4 in Figure 14). However, it might not be possible to clearly detect small channel objects by Landsat-7 ETM+ multi-spectral satellite images, since the ground resolution of these data pixels is 30m.

Wetlands could not be separately discriminated. Since one specific characteristic of these wetlands is the presence of water, they might be included in sub-level classes of the irrigated zone. With more vegetation specific characterization of the wetland class and other context information such as spatial neighbourhood relationship to other known land cover classes, it might become possible to extract those wetland pattern from the satellite image. However, this would then imply shifting the wetland class from the water to the land-natural zone class.

3.5.3 Level III - Land Cover Classification

Land classes at classification level III could mainly be extracted from the irrigation and natural zone (Figure 13). No further discrimination of settlement and infrastructure classes could be achieved. Since Khorezm region is an agricultural region with very little industry, it can be expected that spectral signatures of rural and urban settlements are very similar at the Landsat's spatial ground resolution of 30m. The large ground pixels size compared to smaller real world linear objects might be one spatial reason that obstructed the extraction of roads. Considering multi-spectral reasoning, many small roads in Khorezm are not tarmac, but constructed of compacted soil material, thus spectral reflectance value of roads might be very similar to that of bare soil, such as fields that are prepared for planting.

Irrigation zone classes at level III were mainly discriminated in terms of agriculture and afforestation, while fallow and pasture signatures could not be identified (Figure 13). Those latter LC types might be too small and in between agricultural fields. Pixel with mixed spectral information comprising both agricultural fields, fallow or pastures exacerbate the extraction of homogenous fallow and pasture sites. Afforestations were mainly found close to the Amu Darya River as well as in areas buffering the main and secondary irrigation channels (green signature) where efficient water supply was available.

Natural zone classes at classification level III were identified in terms of natural forest, and bare soil. Bushland was not identified, since that area might be too small to be detected by Landsat image or might consist of a similar spectral signature to other land cover signatures. The forest LC could be found along the river Amu Darya comprising the Tugai forest (dark green signature) (Spot 4 in Figure 14 and Spots 5 and 6 in Figure 15). Bare soil in the form of sand dunes was found in an aggregated spatial pattern in the central part within the irrigation zone and north of the Amu Darya river (Spot 2 in Figure 14). Many fragmented patches of bare soil are distributed within the irrigation zone, which are most likely cotton and rice fields that were prepared for cultivation or where sprouting has not yet taken place. An exact classification of the bare soil fraction might therefore be revealed with land cover classification using an image at an advanced vegetation stage. The desert and desert with some vegetation classes of the land cover classification could be sub-summarized to the bare soil class.

Water channels. Third level water classes were only clearly discriminated in terms of large linear objects. These objects comprised the main drainage (circling the irrigation zone in the south) and the main irrigation channel, branching off the river Amu Darya in a southwestward direction (Spots 1-4 in figure 14). All smaller channel structures could not be extracted due to scaling reasons that were described above.

3.5.4 Level IV - Land Cover Classification

The land cover level IV was used to distinguish different agricultural crops and afforestation types.

Wheat, cotton and rice. Spectral signatures representative for wheat, cotton and rice could be extracted and were mapped in Figure 13. Wheat and cotton fields cover most of the irrigation area and are widely scattered. Rice fields were cultivated in the larger aggregated units in the vicinity of Amu Darya River or in areas buffering the main irrigation channel (mainly Spots 3 and 4 in Figure 14). Smaller rice fields were scattered in the center of the irrigation zone (Spot 2 in Figure 14). Since the training data sets to classify crops were targeted to capture the spectral signatures only from these fields, which already showed at the time of field sampling some crop-specific vegetation reflectance, those cotton and rice fields, in which sprouting was delayed, were automatically classified as bare soil. Delayed sprouting might be due to the combined effects of late planting, inappropriate water supply to crops, soil and water induced salinity stress among other factors. The classification of another Landsat image at the time shortly before cotton and rice harvest would most likely overcome this limitation and extraction of all cotton and rice fields with exact quantification of crop area share are expected.

Maize and legumes. The cultivation of maize and legume occurred mainly in backyard gardens and could therefore not be sensed as a homogenous pattern by Landsat satellite.

Afforestations. In the level IV of the land cover classification scheme afforestation types including shelterbelts, forest patches and orchards were targeted. However, since the same tree type such as poplar is often used both in shelterbelts and forest patches and due to the fact that orchard tree types consisted of a similar spectral signature to the prior two types, no further differentiation of afforestations could be established. Considering the spatial distribution of afforestations, it becomes evident, that they represent only very small area shares in the study region compared to other land cover types such as cotton and wheat (Figure 13). There is a more dense distribution of afforestations in areas close to the Amu Darya River (Spot 4 in figure 14 and Spots 5 and 6 in Figure 15). The same spatial relationship of afforestation occurrences applies to areas buffering the primary and secondary irrigation channels, with again more frequent patterns of afforestation at the head positions of those channels, where efficient water supply is expected (Spots 1-3 in Figure 14).

More detailed scale investigations are expected to provide insight in the spatial arrangement of certain land cover types. These investigations are suited to reveal cross-relationships with already identified leaf area index patterns.

3.6 Comparison of Land Cover Classes and LAI in Selected Spots

The comparison of land cover class distribution and LAI dynamics patterns in selected example spots is presented in Table 3.3.

Table 3.3: Comparison of land cover classes and LAI dynamics in example spots

Spot #	Spatial Location	Conspicuous Land Cover Classes	LAI Dynamics – Land Cover Congruence
1	Upstream, fringe between desert and Khorezm irrigated zone	Desert and desert with some vegetation, transition to cotton cultivation (from SE to NW direction), large settlements, some bare soil patches; small lakes; afforestations (shelterbelts) along the irrigation channel, few rice fields adjacent to the irrigation channel	Very little (0-3) to little (4-9) LAI dynamics in the desert, some fragmented high (20-24) LAI dynamics in afforestations, high-to-moderate (15-19) LAI dynamics in cotton and wheat.
2	Upstream, central area of Khorezm irrigated zone	Bare soil (dunes) clustered in band-like structure, mainly cotton fields followed by wheat fields, few rice fields	Little (9-10) LAI dynamics on bare soil (dunes); moderate (14-10) LAI dynamics on wheat; high-to-moderate (19-15) LAI dynamics in cotton
3	Upstream, close to river area, within the Khorezm irrigated zone	Mainly rice fields adjacent to the irrigation channels and in spatial neighbourhood to wheat and cotton fields; strong presence of orchards and afforestations	Moderate (10-14) LAI dynamics in rice fields; high (20-24) LAI dynamics in afforestations; high-to-moderate (19-15) LAI dynamics in cotton and wheat fields
4	Upstream, directly adjacent to river area, within Khorezm irrigated zone	Mainly rice fields and forest adjacent to the river, while cotton and wheat dominate agricultural land at a greater distance from the river; dark blue signature dominating in the river while bright blue signature increases further downstream	High (20-24) LAI development in rice fields; high-to-moderate (19-15) LAI dynamics in cotton and rice fields; moderate to low dynamics in forest
5	Midstream, directly adjacent to river, adjacent to Khorezm irrigated zone	Mainly forest and some rice adjacent to the river, while cotton and settlements dominate agricultural land at a greater distance from the river; equal contributions of dark blue signature and bright blue signature in the river	High (20-24) LAI development in rice fields; high-to-moderate (19-15) LAI dynamics in cotton fields and moderate (14-10) patterns of LAI dynamics in wheat fields
6	Midstream, directly river overlapping, in Karakalpakstan	Mainly forest and some rice adjacent to the river, while cotton and settlements dominate agricultural land at a greater distance from the river; bright blue signature throughout in the river	Moderate (10-14) LAI dynamics in the forest, Little (4-9) LAI in the desert and rice fields, moderate-to-high (15-19) LAI dynamics in the cotton fields

This descriptive comparison indicates that LAI dynamics of the same land cover class may differ depending on the location of the land cover class as can be shown in Figure 14, e.g. rice fields in spot 3 (Figure 14) have lower LAI dynamics than rice fields in spot 4. That difference might be explained by the fact that spot 4 is located directly adjacent to the river providing optimum water supply throughout the year to respective clustered rice fields. In contrast, rice fields in spot 3 are located in areas buffering the primary and secondary irrigation channels. Since the latter rice fields are fragmented they must share water with other adjacent fields covering cotton, wheat, etc., thus leading to sub-optimal water supply for rice, which in turn may explain the relatively low LAI dynamics. Comparing the occurrence of rice fields from the river to the desert (spots 1 – 4), it is

striking that with greater proximity to the desert fewer and more fragmented rice fields are cultivated. These findings show that proximity to the river or to the main irrigation channels together with clustered field arrangement are likely factors that determine optimum or sub-optimum LAI dynamics for rice cultivation. In contrast, sites closer to the desert, where irrigation networks tend to thin out, show low LAI dynamics for rice.

This reasoning of water body proximity and clustered cultivation to explain LAI dynamics is also applicable to LAI dynamics in afforestations (compare spots 1-4 in Figure 14).

Cotton and wheat cultivations, which are the most widespread crops within the study region, show relatively equally dispersed spatial field arrangement with no preferred cultivation location close to water bodies. Consequently LAI dynamics show no significant changes (compare spots 1-4 in Figure 14). It can be expected that with LAI data at higher spatial resolution, dependencies on the proximity of water bodies might also become evident for cotton and wheat cultivations.

Higher resolution vegetation data might also reveal correlations with other possible determining factors such as ground water salinity, irrigation scheduling, crop management and irrigation channel layout as well as perhaps influence of water institutions.

4 CONCLUSIONS AND OUTLOOK

Multi-temporal and multi-spatial remote sensing data sets from the lower Amu Darya Basin were analysed in terms of spatial and temporal vegetation patterns. Remote sensing data sets that were used in the analysis comprised a MODIS LAI time series for 2002 and one Landsat-7 ETM+ scene from July 12th 2002.

Time series of MODIS LAI data were analysed using descriptive statistics and unsupervised classification. This analysis revealed spatial patterns with maximum, minimum and other LAI development parameters as well as nine different LAI classes with distinct spatial and temporal patterns covering the lower Amu Darya Basin. Example spots were selected to represent areas with varying relative distance to Amu Darya River and to the main irrigation channels. LAI development in these spots mirrored the spatial influence of those water sources. In order to relate LAI to specific land cover types, supervised land cover classification was performed using the Landsat image. The supervised classification led to the demarcation of 13 land cover classes that were structured in a hierarchical classification scheme. LAI development was compared with these land cover classifications. It was possible to relate the spatial pattern of specific land cover classes to specific LAI. Furthermore, it was shown that the LAI dynamics of rice and afforestations were determined by spatial distance relationships to river and irrigation channels as well as by the level of spatial

aggregation of those fields (clustered or dispersed). Cotton and wheat fields that were widely scattered over the study region showed relatively homogenous LAI dynamics.

Explorative LAI development and land cover classification analyses were used as a first step to describe spatial and temporal vegetation and land cover patterns and to derive hypotheses about their determining factors. The most important determining factors for those patterns might include environmental (e.g. water availability, soil salinity, ground water salinity), management (e.g. irrigation scheduling, crop management) and infrastructure (e.g. irrigation channel layout, water institutions) factors.

The next research step could lead to correlation analysis of these factors with LAI parameters in specific land cover classes. Knowledge of temporal development of specific LAI parameters might then allow prediction of LAI development under given environmental, management and infrastructure conditions. These predictions may include determining harvest times for certain crops in specific areas. Information from these predictions of LAI development may also be used to actively control irrigation schedules for certain areas within the irrigation zone during the crop-growing phase. These active management control interventions may help to achieve precise water supply to crops and thus to achieve both optimised crop production and more efficient water use.

Following the correlation and prediction research phase, scenarios of restructured land and water pattern and resource management could be modelled in subsequent study activities to investigate their possible impact on ecological functions (e.g. water requirements for new crops or trees or agro-forestry systems) and economic functions (e.g. crop yield).

Remote sensing data integration from multiple spatial and temporal scales has proved to be well suited for monitoring ecological processes that are related to distinct land cover patterns of large areas such as the lower Amu Darya agro-ecosystem (Mass, 1998; Bastiaanssen and Samia, 2003; El-Magd and Tanton, 2003). The process knowledge that can be inferred from temporal scale analysis may then be used to model and to predict ecological parameters for different spatial land use scenarios. The synergetic use of high temporal and medium spatial resolution with low temporal and high spatial resolution remote sensing products is expected to yield substantial benefits for the upscaling and downscaling of ecological process information over spatial and temporal scales. The usage of these publicly available multi-resolution products for monitoring and prediction of ecosystem functions over space and time may become an important support tool to local policy makers and planners in deciding on ecologically and economically optimised water supply and crop production.

ACKNOWLEDGEMENTS

This study was funded by the German Ministry for Education and Research (BMBF; project number 0339970C). We are especially appreciative to Dr. Christopher Martius and Colin Davenport, Center for Development Research (ZEF) for their thoughtful suggestions and careful review.

REFERENCES

- Bastiaansen W.G.M and S. Ali (2002): A new crop yield forecasting model based on satellite measurements applied across the Indus Basin, Pakistan. *Agriculture, Ecosystems and Environment*, 94, 321-340.
- El-Magd I.A. and T.W. Tanton (2003): Improvements in land use mapping for irrigated agriculture from satellite sensor data using multi-stage maximum likelihood classification. *Int. J. Remote Sensing*, Vol. 24, No. 21, 4197-4206.
- FAO (1997): *Africover Land Cover Classification*. FAO, Rome.
- Freund, J.E. (1992): *Mathematical Statistics*, 5e, New Jersey, Prentice Hall.
- Jansen, J.M. L. and A.D. Gregorio (2002): Parametric land cover and land-use classifications as tools for environmental change detection. *Agriculture, Ecosystems and Environment*, 91, 89-100.
- Knyazikhin, Y., Martonchik, J.V., Myneni, R.B., Diner, D.J. and S.W. Running (1998): Synergistic algorithm for estimating vegetation canopy leaf area index and fraction of absorbed photosynthetically active radiation from MODIS and MISR data. *J. Geophys. Res.*, 32257-32276.
- Mass S.J. (1998) Estimating cotton canopy ground cover from remotely sensed scene reflectance. *Agron. J.* 90, 384-388.
- Myneni, R. B.; Hoffmann, S. et al. (2002): Global products of vegetation leaf area and fraction absorbed PAR from year one of MODIS data. *Remote sensing of Environment* 83: 214-231.
- Lotsch, A., Tian, Y. Friedel, M.A. and R.B. Myneni (2001): Land cover mapping in support of LAI/FPAR retrievals from EOS-MODIS and MISR: classification methods and sensitivities to errors. *Int. J. Remote Sens.* (accepted for publication).
- Shirokova, J. (2000): *Problemy uchudshenia kachestva pochv v usbekistane*. Working Paper, unpublished.
- UNESCO (2000): *Water related vision for the Aral Sea Basin for the year 2025*. UNESCO, Division of Water Sciences with the Co-Operation of the Scientific Advisory Board for the Aral Sea Basin. UN Educational, Scientific and Cultural Organization.
- Vlek, P.L.G., Martius, C., Schoeller-Schletter, A., Wehrheim, P. (2001): *Economic and Ecological Restructuring of Land- and Water Use in the Region Khorezm (Uzbekistan): A Pilot Project in Development Research*. Project Proposal. Bonn.